Coexistence of Universal and Topological Anomalous Hall Effects in Metal CrO_2 Thin Films in the Dirty Limit

W. R. Branford,[1] K. A. Yates,[1] E. Barkhoudarov,[1] J. D. Moore,[1] K. Morrison,[1] F. Magnus,[1] Y. Miyoshi,[1] P. M. Sousa,[2] O. Conde,[2] A. J. Silvestre,[3] and L. F. Cohen[1]

[1]*Physics Department, Blackett Laboratory, Imperial College London, Prince Consort Road, SW7 2BZ, United Kingdom*
[2]*FCUL, Department of Physics and ICEMS, 1749-016 Lisboa, Portugal*
[3]*Instituto Superior de Engenharia de Lisboa and ICEMS, 1959-007 Lisboa, Portugal*

(Received 17 February 2009; published 5 June 2009)

The scaling exponent of 1.6 between anomalous Hall and longitudinal conductivity, characteristic of the universal Hall mechanism in dirty-metal ferromagnets, emerges from a series of CrO_2 films as we systematically increase structural disorder. Magnetic disorder in CrO_2 increases with temperature and this drives a separate topological Hall mechanism. We find that these terms are controlled discretely by structural and magnetic defect populations, and their coexistence leads to apparent divergence from exponent 1.6, suggesting that the universal term is more prevalent than previously realized.

DOI: 10.1103/PhysRevLett.102.227201 PACS numbers: 75.47.−m, 72.15.Gd, 72.25.Ba, 85.75.−d

The anomalous Hall effect (AHE) has been investigated extensively in ferromagnetic (FM) metals [1]. It has been described empirically as being proportional to the magnetization of a sample, giving a total Hall resistivity of $\rho_{xy} = R_O B + R_S \mu_0 M$, where R_O and R_S are the ordinary and anomalous Hall coefficients, respectively, and $\mu_0 M$ is the magnetization. Theory and recent experiments show [2–4] that this is part of a much more general phenomenon, the spin Hall effect, that describes a transverse deflection of current carriers, and produces a spatial separation of spin currents [3,5]. This spin Hall term can arise from either intrinsic or extrinsic processes and requires only the presence of spin-orbit coupling. In ferromagnetic metals, the quantity of spin-up and spin-down charge carriers are unequal and so this spin separation has an associated charge imbalance which is detected as an anomalous Hall (AH) voltage.

It has recently been established that there is a large window in conductivity and materials space where a scaling relationship between the anomalous Hall conductivity (σ_{AH}) and the longitudinal conductivity $(\sigma_{xx})^{1.6}$ holds [6–9]. The relationship is known as universal scaling and the theoretical work [8] that first proposed this phenomenon defined a restricted parameter space where a resonant enhancement of the intrinsic AHE term in a multiband FM ''dirty-metal'' occurs. In a dirty metal the structural point-defect density strongly influences the scattering time, τ_h. The parameter space for resonant AHE requires that the Fermi level is located close to an anticrossing of band dispersions split by spin-orbit interaction, $\varepsilon_{\mathrm{SO}}$ (a topological singularity in momentum space). The theory [8] proposed that a crossover from extrinsic to intrinsic AHE is triggered by a resonance condition when the two key energy scales in the model $\hbar/\tau_h$ and $\varepsilon_{\mathrm{SO}}$ become comparable. Interestingly, band structure calculations on CrO_2 [10] show that it can satisfy the restricted universal scaling criteria, yet experimentally it is already known to exhibit a separate intrinsic AH mechanism driven [11] by the topological gauge field that emerges with a thermal population of purely magnetic defects. Furthermore, it is an unusual system with good-metal-like residual resistivity, RR $\sim 2 \times 10^{-8}$ Ω m, at base temperature [12], and strong T^2 temperature dependence to the resistivity (ρ) above 100 K associated it is thought, with half-metallicity [12,13]. The $\rho(T)$ behavior has previously created a difficulty in distinguishing conductivity and temperature-dependent effects such as magnetic gauge field strength. We address this point by growing polycrystalline films on lattice mismatched Al_2O_3 substrates, where the strain induced defects produce a RR that is at least an order of magnitude higher than for single crystalline films [14]. The level of dirtiness is controlled systematically by decreasing film thickness, isolating conductivity dependent effects from thermal effects, and revealing universal Hall scaling [6–9] in CrO_2. In this Letter we demonstrate that the universal-scaling term can be controlled by modifying the structural defect population and hence the carrier scattering time. We also find that the topological Hall term can be separately controlled by the pure magnetic defect concentration, which varies exponentially with temperature. Above 100 K we find coexistence of the universal-scaling term and the topological term. These parallel Hall conductance pathways lead to an apparent divergence of the raw data from the universal exponent of 1.6 at higher temperatures. We are able to fit the data robustly to a two-channel model with universal and topological terms, which demonstrates that the universal scaling with exponent 1.6, observed across a wide range of materials is a property of the specific Hall mechanism, rather than a fundamental relationship between Hall and longitudinal transport.

Films studied in this Letter were grown on Al_2O_3 (0001) by chemical vapor deposition at 380 °C with an O_2 flux of

50 sccm [15] with deposition times of 4, 2 and 1 h. A film grown at 330 °C for 8 h is also used in this study. X-ray diffraction measurements suggest that the CrO_2 material within the grains of each film appears to be of a similar structural quality. However, the thinner films exhibited a buffer layer of (antiferromagnetic insulator) Cr_2O_3 at the CrO_2/Al_2O_3 interface. The effective transport thicknesses of these CrO_2 films, as determined by cross-sectional scanning electron microscopy and corrected for Cr_2O_3 interface layer thickness as determined from x-ray diffraction and vibrating sample magnetometry, were 595, 251 and 39 nm, respectively, for the 380 °C grown films and 62 nm for the film grown at 330 °C. The morphology of the films consists of large (micron-sized) equiaxial particulates which are composed of a number of elongated grains. The particle size increases markedly with thickness [16]. The grain size measured by x-ray diffraction increased with deposition temperature from 33 nm at 330 °C to 80 nm at 380 °C [16]. Films grown by this method have been extensively characterized [15–18], point contact Andreev reflection measurements on the 595, 251 and 62 nm films in this study were published previously [17], confirming bulk spin polarization of the transport carriers (P_t) close to 100% and no strong correlation with morphology.

Magnetotransport data were collected in a square geometry with standard four-point techniques. The methodology used to extract the Hall parameters from magnetic and transport measurements is described in detail elsewhere [19]. The saturation magnetization determined from magnetization vs field loops is shown as a function of temperature in Fig. 1(a). The temperature dependence is similar to the bulk for all of the films indicating that the CrO_2 has similar magnetic properties across the series, with $T_C \sim 386$ K [20] although T_C appears to be somewhat reduced in the thinnest film. Figure 1(b) shows the resistivity versus temperature. The resistivity ratio varies from 15 for the 595 nm film to 3.3 for 39 nm film. The RR of the 595 nm film grown at 380 °C is in good agreement with other thick films grown on Al_2O_3 (0001) [14] whereas the thinner films have a RR that is greater by up to an order of magnitude. The increasing RR with decreasing thickness films shows increased defect scattering as interface strain becomes more important, whereas the magnitude of the thermal term in the resistivity is similar for all samples. The two thinner films fall in the dirty regime as we have defined it, and the thicker two in the intermediate regime.

Figure 1(c) shows the Hall resistivity versus field at selected temperatures for the 251 nm film as an example of the raw data. An iterative procedure was used to fit the measured Hall resistivity to the expression $\rho_{xy} = R_O B + R_S \mu_0 M$. R_O was found to be field independent and positive for all films at all temperatures studied, consistent with single carrier, hole-mediated transport at all temperatures. Note that we do not find a "two-carrier" type crossover behavior as observed by Watts *et al.* [21].

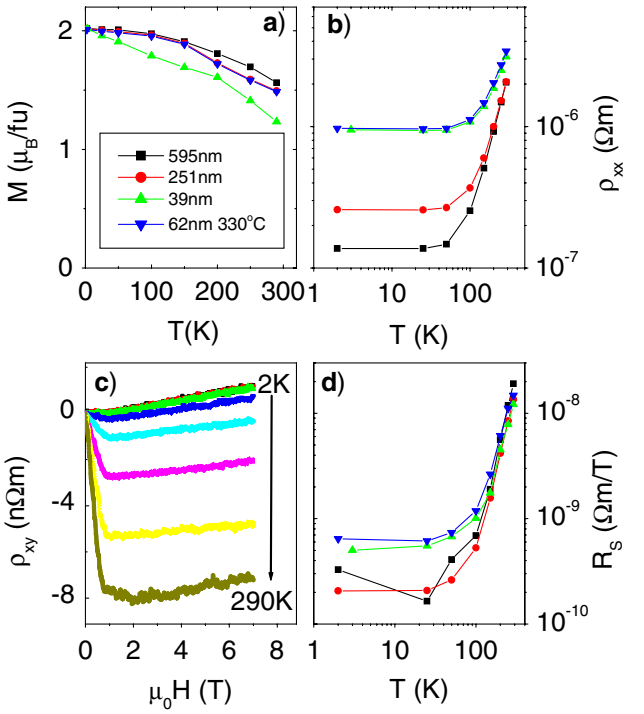

FIG. 1 (color online). (a) Saturation magnetization vs T. (b) Resistivity vs T. (c) Hall resistivity vs field of 251 nm film at 2 K, 25 K, 50 K, 100 K, 150 K, 200 K, 250 K and 290 K. (d) Anomalous Hall constant vs T [symbols as in (a)].

We now turn to the AH data. The AH constant R_S is plotted versus temperature in Fig. 1(d). R_S is negative for all films at all temperatures. In a "clean limit" sample R_S was previously [11] fit to the function $R_S = (A/T) \times \exp(-E_C/k_B T)$ which tends to zero as T tends to zero, which is clearly not sufficient to describe our data.

The hole mobility and the carrier concentration (in the inset), determined from R_O for all the films is shown in Fig. 2. The carrier hole mobility decreases with film thick-

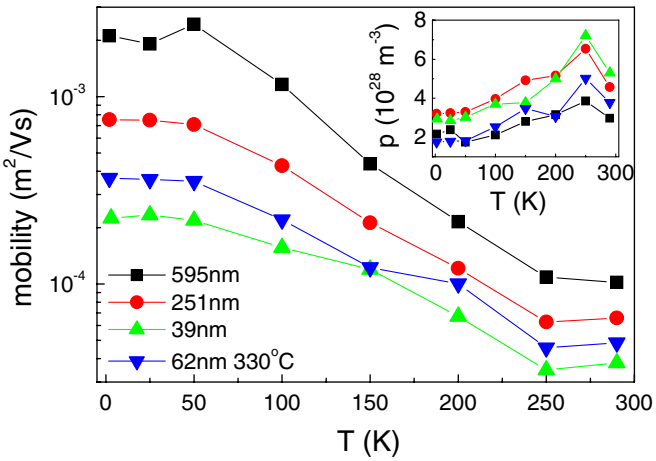

FIG. 2 (color online). Hole mobility vs T and (inset) hole concentration vs T.

ness, and we attribute this to increased defect scattering as interface strain dominates. The mobility also decreases strongly above 100 K once the T^2 term becomes significant in the resistivity. If one assumes a crude single (majority) carrier model such that $\mu_h = e\tau_h/m_h^*$ and hole scattering length $l_h = \tau_h\langle v_h\rangle$ and takes $m_h^* = 10m_e$ [22] and $\langle v_h\rangle = 2.2 \times 10^5$ m/s [23] then one obtains a hole scattering time of $\tau_h = 120$ fs and a scattering length of 26 nm for the 595 nm film. In the 39 nm film $l_h = 2.8$ nm and $\tau_h = 13$ fs. For comparison the scattering length in single crystal CrO_2 is 70 nm [23]. The average grain size in the films grown at 380 °C (330 °C) is around 80 nm (33 nm). This is a useful guide to the relevant length scales and suggests that the increased RR reflects changes in the intragrain transport, strain effects caused by the lattice mismatch rather than a grain boundary effect. The hole concentration, shown in the inset to Fig. 2, is much less sensitive to film thickness and increases with temperature.

The saturation AH conductivity, σ_{AH} derived from this data ($\sigma_{AH} = \rho_{xy,sat}/{\rho_{xx}}^2$), is plotted as a function of σ_{xx} in Fig. 3. Here we isolate σ_{xx} dependent effects from thermal effects by grouping the data by temperature, rather than by sample. The lines show fits to $|\sigma_{AH}| = C{\sigma_{xx}}^{\alpha} + D$, and the exponent calculated at each temperature is plotted in the inset, with $\alpha \sim 1.6$ below 100 K and increases gradually to $\alpha > 2$ at room temperature.

Now let us attempt to construct a full description of σ_{AH} for our films. For epitaxial CrO_2 films on TiO_2 with very low RR (2×10^{-8} Ω m) it has been found that σ_{AH} can be described [11] by a topological term. The topological model describes a thermal population of purely magnetic defects. At finite temperatures the "perfect" collinear FM order starts to break up, with the defects being magnetic monopoles with magnetic charge $Q = \pm 1$. These monopoles are unstable with respect to a $+-$ defect pair on neighboring lattice sites, described as a skyrmion string. The population of these defect pairs $\langle n_d\rangle$ is described by a core energy, E_C, with $\langle n_d\rangle \propto \exp(-E_c/k_BT)$. The pairs carry a net dipole moment which interacts with the magnetization, M. The perturbation to the pair energy by this interaction is described by a string spin-orbit energy, λ_{so} such that $\langle {n_d}^{\pm}\rangle \propto \exp[(\pm\lambda_{so} - E_c)/k_BT]$. A finite λ_{so} results in an imbalance of aligned and antialigned skyrmion strings and a gauge field $\langle b_z\rangle$ emerges. The magnetic topology causes a Berry phase shift of the charge carriers, resulting in an anomalous transverse velocity of the carriers and a measurable Hall voltage. In the films studied here we find that we have to invoke both the universal and topological models in order to describe the data, and that quite remarkably, the two mechanisms appear to operate in parallel. Having demonstrated that the universal scaling exponent of 1.6 applies to the CrO_2 system at low temperature, we now extract thermally activated AH effects associated with the gauge field as the deviation from the universal behavior as the temperature is increased.

Figure 4(a) shows σ_{AH} vs temperature and a fit of the data to a two component model. At 2 K our films obey the

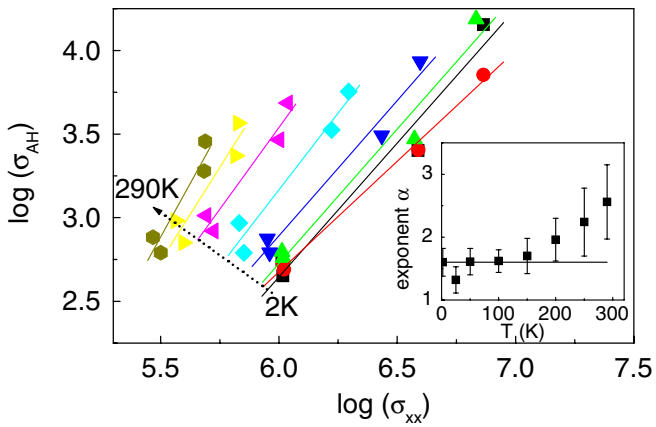

FIG. 3 (color online). (Data grouped by temperature, not sample, $\sigma_{AH} = \rho_{xy,sat}/{\rho_{xx}}^2$). $|\sigma_{AH}|$ vs σ_{xx} at 2 K, 25 K, 50 K, 100 K, 150 K, 200 K, 250 K and 290 K (symbols) and fits to $|\sigma_{AH}| = C{\sigma_{xx}}^{\alpha} + D$ (lines). Inset: Best-fit exponent α vs T (symbols) and $\alpha = 1.6$ (line).

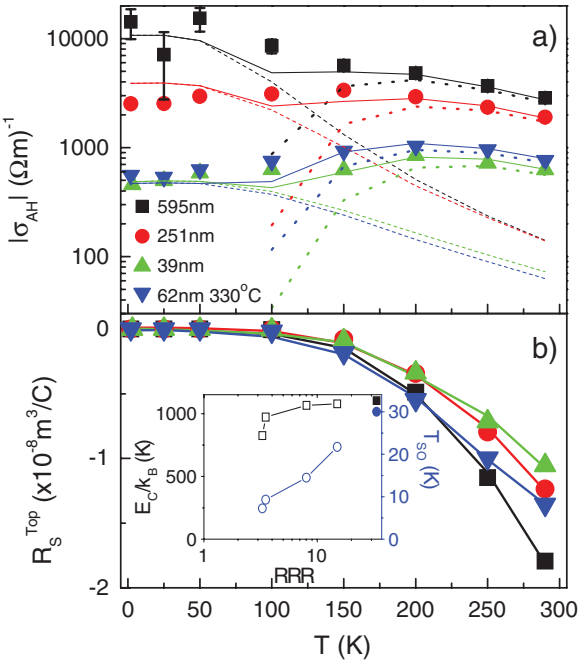

FIG. 4 (color). (a) Measured saturation anomalous Hall conductivity vs T (symbols). Dashed line: ${\sigma_{AH}}^{U,calc}(T) = 1.1 \times 10^{-7}(\Omega\,\mathrm{m})^{0.6}(\sigma_{xx}(T))^{1.6}$. Dotted line: ${\sigma_{AH}}^{Top,calc}(T) = [\mu_0 M_S(T)\cdot(\sigma_{xx}(T))^2]\cdot(A/T)\exp(E_C/k_BT)$. Solid line: ${\sigma_{AH}}^{Calc}(T) = {\sigma_{AH}}^{U,calc}(T) + {\sigma_{AH}}^{Top,calc}(T)$. (b) Topological Hall constant, ${R_S}^{Top}(T) = {\sigma_{AH}}^{Top}(T)/[\mu_0 M_S(T)\cdot(\sigma_{xx}(T))^2]$ (symbols) and fit to ${R_S}^{Top}(T) = (A/T)\exp(E_C/k_BT)$ (lines). Inset: Magnetic defect pair core temperature (squares) and spin-orbit temperature $T_{SO} = \lambda_{SO}/k_B$ (circles) vs residual resistivity ratio; open symbols are this work, closed symbols are taken from Ref. [11].

universal scaling $|\sigma_{AH}| = C\sigma_{xx}^{1.6} + D$, with $C = 1.1 \times 10^{-7}$ $(\Omega\,\mathrm{m})^{0.6}$. In many materials this scaling is valid from base temperature to room temperature despite dramatic changes in conductivity and conduction mechanism [6,7]. Therefore, we define a universal term which is shown as the dashed lines in Fig. 4(a), $\sigma_{AH}^{U}(T) = 1.1 \times 10^{-7}$ $(\Omega\,\mathrm{m})^{0.6}(\sigma_{xx}(T))^{1.6}$. We now assume that the deviation from the universal behavior is caused by the topological term, $\sigma_{AH}^{Top}(T)$ where $\sigma_{AH}^{Top}(T) = \sigma_{AH}^{Meas}(T) - \sigma_{AH}^{U}(T)$. Figure 4(a) shows the variation of the topological term $\sigma_{AH}^{Top,calc}(T)$ as a dotted line. We then convert to a topological Hall constant $R_S^{Top}(T) = \sigma_{AH}^{Top}(T)/[\mu_0 M_S(T) \cdot (\sigma_{xx}(T))^2]$ and fit to $R_S^{Top}(T) = (A/T) \times \exp(E_C/k_B T)$ as shown in Fig. 4(b). The inset to Fig. 4(b) shows the magnetic defect pair core temperature, E_C/k_B, and spin-orbit interaction temperature, λ_{so}/k_B, obtained from this fitting procedure vs residual resistivity ratio (RRR $= R_{290\,K}/R_{2\,K}$). In the clean limit Yanagihara *et al.* [11] found $E_C/k_B = 1103$ K $\pm$ 28 K and $\lambda_{so}/k_B =$ 30 K. Data taken from Ref. [11] are shown for comparison in the inset to Fig. 4(b) along with the defect core temperature and spin-orbit temperature vs RRR from our own data. The spin-orbit temperature appears approximately linear with the RRR while the core temperature is nearly constant, only starting to decline in the dirtiest films. A calculated topological AH conductivity, $\sigma_{AH}^{Top,calc}$, can be generated for each film using these extracted parameters and the measured M_S and σ_{xx} using $\sigma_{AH}^{Top,calc}(T) = [(\mu_0 M_S(T)\sigma_{xx}(T)^2) \cdot (A/T)\exp(E_C/k_B T)]$, shown as the dotted lines in Fig. 4(a): The total calculated two term AH conductivity model, $\sigma_{AH}^{Calc}(T) = \sigma_{AH}^{U,calc}(T) + \sigma_{AH}^{Top,calc}(T)$ is shown by solid lines in Fig. 4(a). This function describes the measured data well at all temperatures.

An interesting aspect of the work is the effect that moving from the clean to the dirty transport limit has had on the temperature dependence of σ_{AH}. In samples in the dirty limit, the σ_{AH} is only weakly temperature dependent, which corresponds to our earlier observations on Co_2MnSi [19] and strongly suggests that the transport spin polarization is robust up to room temperature. In the thicker films, in the intermediate-dirty limit the AH was a strong function of temperature, but a temperature dependent P_t was not required to fit the data, and again P_t appears robust.

In summary, we find that the carriers in films studied here are holelike, the hole mobility correlating with film thickness and the residual resistivity ratio governed by carrier mobility, not carrier density. CrO_2 has the band features required for the resonant mechanism and by growing a series of films with systematically increasing structural defect concentration, or dirtiness, at a given temperature, we are able to isolate the universal Hall scaling. CrO_2 also exhibits a topological Hall term that is controlled by the concentration of purely magnetic defects, and above 100 K we observe coexistence of the universal and topological terms with an apparent deviation from the exponent 1.6. We note that both of these terms are intrinsic, and yet one increases and the other is suppressed by the concentration of certain defects. Furthermore, both have a quantum topological aspect and we observe coexistence of topological singularities in real and momentum space in CrO_2. An additional observation relates to spin polarization of the carriers. We have previously reported that the transport spin polarization of these films is not sensitive to the morphological changes in this series of films at 4.2 K and that P_t (4.2 K) is high and close to 90%. The results presented here support this view, moreover, we see no signature to suggest a strong temperature dependence of P_t. This null result is encouraging for spintronic applications suggesting that the spin polarization is robust in this system up to room temperature. The requirements to engineer this effect in other systems are spin-orbit splitting of magnetic defects, strong coupling of carriers to local magnetic moments and possibly half-metallicity. As these conditions are met in the manganite system, it is possible that the manganites would display similar tunability of properties.

This work was funded by the UK EPSRC and PT FCT (Contract No. POCTI/CTM/41413 and PhD funding to P. M. S.).

[1] C. M. Hurd, *The Hall Effect in Metals and Alloys* (Plenum Press, New York-London, 1972).
[2] J. E. Hirsch, Phys. Rev. Lett. **83**, 1834 (1999).
[3] Y. K. Kato *et al.*, Science **306**, 1910 (2004).
[4] J. Wunderlich *et al.*, Phys. Rev. Lett. **94**, 047204 (2005).
[5] V. Sih *et al.*, Nature Phys. **1**, 31 (2005).
[6] A. Fernandez-Pacheco *et al.*, Phys. Rev. B **77**, 100403(R) (2008).
[7] T. Fukumura *et al.*, Jpn. J. Appl. Phys. **46**, L642 (2007).
[8] S. Onoda, N. Sugimoto, and N. Nagaosa, Phys. Rev. Lett. **97**, 126602 (2006).
[9] K. Ueno *et al.*, Appl. Phys. Lett. **90**, 072103 (2007).
[10] I. I. Mazin, D. J. Singh, and C. Ambrosch-Draxl, Phys. Rev. B **59**, 411 (1999).
[11] H. Yanagihara and M. B. Salamon, Phys. Rev. Lett. **89**, 187201 (2002).
[12] K. Suzuki and P. M. Tedrow, Phys. Rev. B **58**, 11 597 (1998).
[13] H. C. Jeon *et al.*, Appl. Phys. Lett. **89**, 112517 (2006).
[14] X. W. Li *et al.*, J. Appl. Phys. **85**, 5585 (1999).
[15] P. M. Sousa, Ph.D. thesis, University of Lisbon, 2008.
[16] P. M. Sousa *et al.*, CVD **13**, 537 (2007).
[17] K. A. Yates *et al.*, Appl. Phys. Lett. **91**, 172504 (2007).
[18] P. M. Sousa *et al.*, CVD **12**, 712 (2006).
[19] W. R. Branford *et al.*, New J. Phys. **9**, 42 (2007).
[20] F. Y. Yang *et al.*, Phys. Rev. B **63**, 092403 (2001).
[21] S. M. Watts *et al.*, Phys. Rev. B **61**, 9621 (2000).
[22] L. L. Chase, Phys. Rev. B **10**, 2226 (1974).
[23] S. P. Lewis, P. B. Allen, and T. Sasaki, Phys. Rev. B **55**, 10 253 (1997).